

## Ground-state properties and magnetic excitations of the mixed valence state: Cerium-based alloys

B. H. Grier\* and R. D. Parks

*Department of Physics, Polytechnic Institute of New York, Brooklyn, New York 11201*

S. M. Shapiro and C. F. Majkrzak

*Brookhaven National Laboratory, Upton, New York 11973*

(Received 20 April 1981)

Both the static and dynamic magnetic behavior of the mixed valence system,  $\text{Ce}_{0.9-x}\text{La}_x\text{Th}_{0.1}$ , have been studied through magnetic susceptibility and inelastic neutron scattering experiments. For small La concentrations ( $x \leq 0.09$ ), the system exhibits a first-order valence transition to a strongly mixed valent ground state, whereas nearly integral valent, local moment behavior results for  $x \geq 0.4$ . For the strongly mixed valent system  $\text{Ce}_{0.74}\text{Th}_{0.26}$ , the inelastic neutron spectra are characterized by a broad quasielastic peak, while for  $x \geq 0.14$  in the  $\text{Ce}_{0.9-x}\text{La}_x\text{Th}_{0.1}$  system, the mixed valence effects are weaker and crystalline electric field excitations begin to appear. This occurs when the spin-fluctuation energies associated with the mixed valent state are smaller than the crystal-field excitation energy. Simple relationships emerge which connect various energy-related parameters, namely, the valence transition temperature, the Fermi liquid susceptibility at  $T=0$  and the ground-state spin-fluctuation energy as measured in the neutron scattering experiments.

### I. INTRODUCTION

There is strong and growing interest in the study of mixed valence effects in rare-earth systems,<sup>1-4</sup> and, to a lesser extent, in actinide systems.<sup>4</sup> The anomalous behavior of these systems results from the presence of localized electronic states ( $4f$  in the case of rare earths and  $5f$  in the case of actinides) very close to the Fermi level. (From this point forward we shall restrict our discussion to rare-earth systems.) The above described situation allows for fluctuations of the electrons between the  $4f$  level and the ( $5d,6s$ ) conduction band, resulting in fluctuations of the local ionic configuration between  $4f^n$  and  $4f^{n-1}$ . Such a description was the one initially advanced ten years ago by Hirst.<sup>5</sup>

These fluctuations have a pronounced effect on the physical properties of the system. For instance, if one of the two ionic states is magnetic, the valence fluctuations effectively quench the local moment and the system displays an enhanced temperature-independent Pauli susceptibility at low temperatures. The magnitude of this susceptibility is expected to be inversely proportional to the  $4f$ -( $5d,6s$ ) hybridization energy  $\Gamma$ .<sup>6</sup> At higher temperatures ( $kT \gtrsim \Gamma$ ) the system displays Curie-Weiss paramagnetism with a Curie constant which is

depressed from the value expected if the ions were in a completely stable magnetic configuration. The short lifetime of the spins in mixed valent systems also leads to a broad quasidelectric peak in the neutron inelastic cross section.<sup>7-9</sup> Prior to the present study, crystalline electric field (CEF) transitions had not been observed, as far as we can determine, in neutron scattering studies of mixed valent systems, and had been generally ignored in most theoretical treatments.

We report here the results of measurements of the static and dynamic magnetic properties of the mixed valent alloy system  $\text{Ce}_{0.9-x}\text{La}_x\text{Th}_{0.1}$ , as determined from dc susceptibility and inelastic neutron scattering studies.<sup>10</sup> This system was chosen for the study because of the wide range of behavior displayed. The presence of thorium is for the purpose of stabilizing the fcc phase against parasitic encroachment of the hexagonal  $\beta$  phase, which plagues experiments on elemental cerium.

The  $\text{Ce}_{0.9-x}\text{La}_x\text{Th}_{0.1}$  alloy system, like many other Ce alloy systems, displays a first-order valence transition<sup>11</sup> for small  $x$ . The transition is from the weakly mixed valent (Ce valence  $\eta \sim 3.1$ )  $\gamma$  phase at high temperature to the strongly mixed valent ( $\eta \sim 3.7$ )  $\alpha$  phase at low temperature. Both phases have the same fcc crystal structure. As the

La concentration is increased, the transition temperature decreases from  $T_0 = 140$  K for  $x=0$ . The first-order jump also decreases such that the transition becomes second order at the critical concentration,  $x=0.094$ . For  $x > 0.094$  the transition is continuous. A plot of the transition temperature  $T_0$  (taken to be the midpoint of the hysteresis in the first-order samples and the inflection point in the static susceptibility for the second order and continuous samples) versus  $x$  is shown in Fig. 1. An attractive feature of the system is that  $T_0$  varies by more than an order of magnitude in the range  $0 \leq x \leq 0.2$ , indicating a large variation in the relevant energy parameter(s).

## II. SAMPLE PREPARATION

The  $\text{Ce}_{0.9-x}\text{La}_x\text{Th}_{0.1}$  samples were prepared in the range  $0 \leq x \leq 0.4$  in various shapes and sizes by arc melting the pure materials in an argon atmosphere. The cerium and lanthanum used were obtained from Rare Earth Products Limited and were nominally 99.99% pure. The thorium purity was given as 99.9% with respect to metals by the manufacturer, ALFA Division of Ventron Corporation.

The raw materials were melted together, flipped and melted again. This was repeated until the samples had been melted 10–12 times. Finally, the samples were cast into the shape required. Susceptibility samples (0.9 g) were shaped into approximate 6-mm-diam spheres by melting them

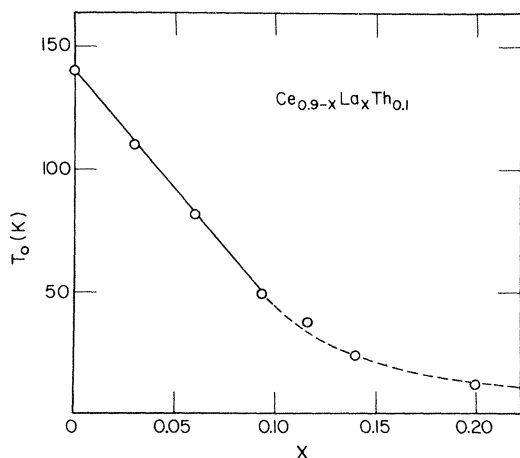


FIG. 1. Phase diagram of the  $\text{Ce}_{0.9-x}\text{La}_x\text{Th}_{0.1}$  alloy system. The lines are drawn as guides to the eye. The solid line denotes first-order transitions while the dashed line represents continuous transitions.

into a 6-mm hemispherical depression in the hearth. Neutron scattering samples (15 g) were shaped into approximate  $0.9 \times 4.4 \times 0.6$  cm<sup>3</sup> elliptical boules by casting them into a suitably shaped depression. Each sample was then wrapped in tantalum foil, sealed in an evacuated quartz tube, and annealed overnight at between 750 and 800°C before being quenched in brine. Since weight loss at each step was negligible, the sample concentration was determined from the weights of the constituents prior to the first melt.

A reliable test of sample quality comes from the neutron diffraction data. Four samples have been tested in this way:  $\text{Ce}_{0.76}\text{La}_{0.14}\text{Th}_{0.10}$ ,  $\text{Ce}_{0.7}\text{La}_{0.2}\text{Th}_{0.1}$ ,  $\text{Ce}_{0.5}\text{La}_{0.4}\text{Th}_{0.1}$ , and  $\text{La}_{0.9}\text{Th}_{0.1}$  and none showed any sign of inhomogeneities. All four were also shown to be predominantly single phase fcc structure, although a small concentration (< 5%) of another fcc phase with lattice constant 5.60 Å was detected in each sample. This additional phase has been observed previously<sup>12</sup> in cerium and cerium alloys and has been attributed to either  $\text{ThO}_2$  or  $\text{CeH}_2$ . There was no detectable evidence of the presence of a hexagonal phase in any of the three samples. The above evidence suggests that all of the samples studied were homogeneous and predominantly single phase.

## III. STATIC MAGNETIC SUSCEPTIBILITY

### A. Low-temperature results (Fermi-liquid behavior)

Static magnetic susceptibility measurements were made by the Faraday method using a Cahn RG electrobalance which was calibrated using a platinum sphere. The measured susceptibilities were then corrected for La and Th contributions. The Th contribution was taken to be temperature independent and equal to  $0.383 \mu\text{emu/g}$  (Ref. 13) and a quadratic fit to the fcc lanthanum susceptibility of Spedding and Croat<sup>14</sup> was used to correct for the La contribution. The sum of the Th and La contributions was always less than  $0.5 \mu\text{emu/g}$  Ce. The resulting values were then corrected at low temperatures for impurities and untransformed  $\beta$ - and  $\gamma$ -cerium which reside presumably in grain boundaries and other strained regions.

Assuming that the low-temperature susceptibility contributions from impurities and trivalent cerium is inversely proportion to  $T$  and the susceptibility of  $\alpha$ -Ce at low temperatures is temperature independent,<sup>15</sup> we have the following trial form for the low-temperature susceptibility

$$\chi(T) = \chi_0 + \frac{B}{T}, \quad (1)$$

where  $\chi_0$  is the intrinsic temperature-independent susceptibility. A previous study of the  $\text{Ce}_{1-x}\text{Th}_x$  alloy system indicated that there may be a constant contribution<sup>16</sup> to the impurity susceptibility as well as the term proportional to  $1/T$ . A subsequent study of the same system<sup>17</sup> showed no evidence for such a term. To further investigate the existence of this term, we have made four low-temperature runs on a single sample (9.35 at. % La). While the  $T^{-1}$  term varied considerably from run to run, there was much less variation in the constant contribution. Furthermore, there seems to be no correlation between the variations in the two terms. Therefore, we find no evidence for any impurity contribution other than the term proportional to  $T^{-1}$ . Another question which often arises is whether the susceptibility of  $\alpha$ -Ce is indeed finite at  $T=0$  or whether at least part of the divergence at low  $T$  is an intrinsic effect, rather than totally an impurity effect. The relationship between the nonsingular part of the low-temperature susceptibility and the other properties of the system in this study indicate that  $\chi_0$  is certainly an intrinsic property of the system. However, susceptibility measurements alone cannot determine whether or not the entire  $T^{-1}$  term is impurity related. Neutron scattering measurements on the other hand provide an independent measure of  $\chi(T)$  where the impurity contribution is negligible. The measurements reported in Sec. IV C imply that the entire  $T^{-1}$  term is impurity related in the systems studied, confirming that the intrinsic low-temperature static susceptibility is indeed temperature independent and equal to  $\chi_0$ . To correct for the impurities, the low-temperature data were fit to Eq. (1) and the  $T^{-1}$  term was subtracted leaving the fully corrected cerium susceptibility. The representative temperature dependence is shown (for the 6 at. % sample) in Fig. 2. Susceptibility curves showing valence transitions of varying strengths are shown in Fig. 3 for several representative samples. The dashed lines are the susceptibilities as measured and corrected for La and Th contributions and the solid lines are after correction for impurities and untransformed cerium. One goal of the present study was to correlate the Fermi-liquid parameters, e.g.,  $\chi_0$ , with various energy parameters of the system. It is predicted that  $\chi_0$  should vary inversely as the  $4f$ -( $5d,6s$ ) hybridization energy  $\Gamma$  (e.g., Ref. 6). In the  $\text{Ce}_{0.9-x}\text{La}_x\text{Th}_{0.1}$  system, the valence transition temperature varies widely as a function

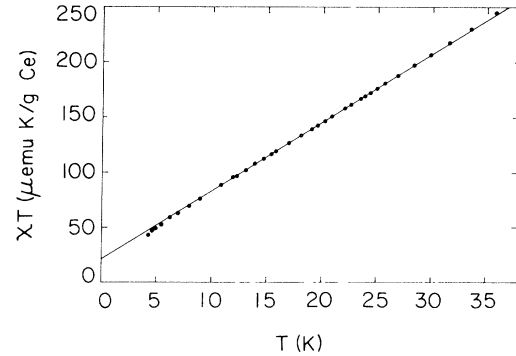


FIG. 2. Product of the susceptibility and the temperature vs the temperature for the 6 at. % lanthanum sample at low temperature. The line is a least squares fit to the form  $\chi T = AT + B$  as discussed in the text.

of  $x$  and so it is expected that  $\Gamma$  should also vary as  $x$  is changed. In fact, our measurements show that  $\chi_0$  varies by more than an order of magnitude from the value for pure cerium. The value of  $\chi_0$  is very simply related to the transition temperature in this system as can be seen in Fig. 4, where we have plotted  $\chi_0$  vs  $T_0$  on a log-log plot. The transition temperature  $T_0$  was taken to be the midpoint of the hysteresis in the susceptibility in the first-order samples ( $x < 0.094$ ) and the inflection point in the susceptibility for the second order and continuous samples ( $0.094 \leq x \leq 0.20$ ). The solid line in the figure is a least-square fit to the form  $\chi_0 = AT_0^{-1}$  which resulted in the value  $A = 515 \pm 7 \mu\text{emu K/g Ce}$ , or  $A = C_0/11.2$ , where  $C_0 = 5760 \mu\text{emu K/g Ce}$  is the free-ion Curie constant for cerium.

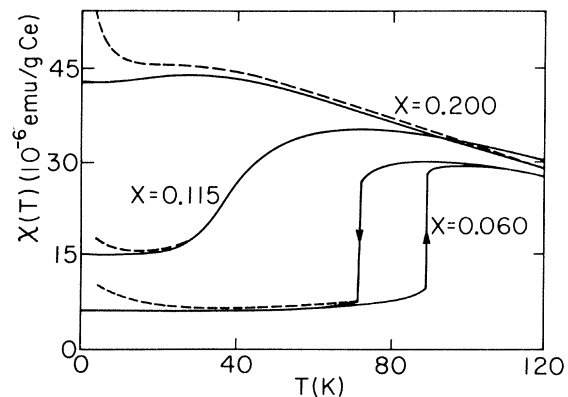


FIG. 3. Dashed lines: measured static magnetic susceptibilities after subtraction of Th and La contributions for three compositions of  $\text{Ce}_{0.9-x}\text{La}_x\text{Th}_{0.1}$ . Solid lines: corrected susceptibilities after subtraction of impurity tail (see text).

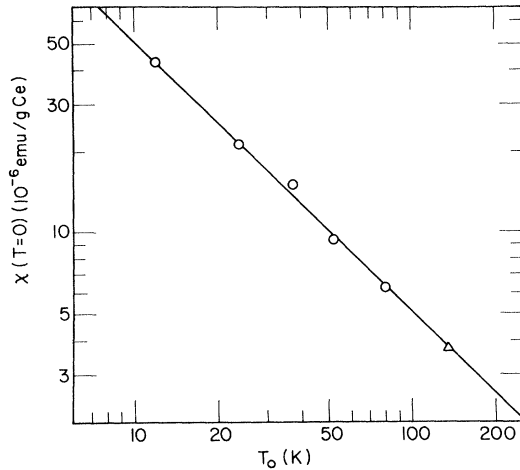


FIG. 4. Asymptotic  $T \rightarrow 0$  susceptibility vs valence transition temperature. Triangle: pure  $\alpha$ -cerium after D. C. Koskenmaki and K. A. Gschneidner, Jr., Phys. Rev. B **11**, 4463 (1975). Circles: different compositions of  $\text{Ce}_{0.9-x}\text{La}_x\text{Th}_{0.1}$  ranging from  $x=0.06$  to 0.20 (this work). Solid line: plot of  $\chi(0) = C_0/11.2T_0$ , where  $C_0$  is the free-ion Curie constant.

This dramatic decrease of the  $f$ -level hybridization can be understood from the results of the study by Manheimer<sup>18</sup> concerning the effects of the size and valence of lanthanum on the transition temperature. Lanthanum is larger than both trivalent and (hypothetical) tetravalent cerium and so acts as a negative pressure in the alloy, lowering the  $f$  level with respect to the Fermi level. Trivalent lanthanum also contributes fewer electrons to the conduction band than does mixed valent cerium. As suggested in Ref. 18, this probably decreases the screening of the  $f$  electrons from the nucleus and leads to a more localized and more tightly bound cerium  $f$  electron. Thus both the size and valence effects associated with the La additive act to decrease the amount of hybridization with the conduction band.

### B. High-temperature results

In his studies of the  $\text{CeIn}_{3-x}\text{Sn}_x$  system, Lawrence<sup>19</sup> found that the susceptibility curves could be scaled by a single parameter which he called  $T_{\text{SF}}$ , with  $\chi T$  vs  $T/T_{\text{SF}}$  being independent of  $x$  for a large range of  $x$  and  $T$ . A similar scaling occurs at low temperature in the  $\text{Ce}_{0.9-x}\text{La}_x\text{Th}_{0.1}$  system. A plot of  $\chi T$  vs  $T/T_0$  is shown in Fig. 5 for several values of  $x$ . Since the susceptibility is constant and inversely proportional to  $T_0$ , a plot of

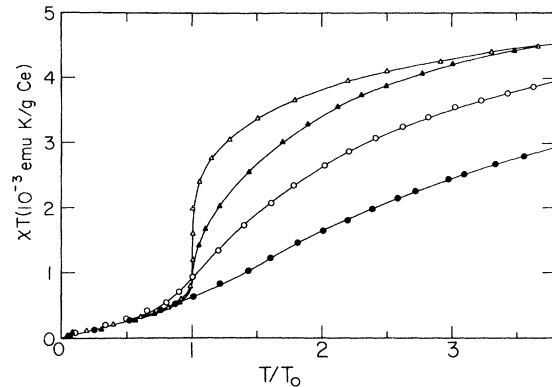


FIG. 5. Susceptibility times the temperature vs scaled temperature for four samples with the formula  $\text{Ce}_{0.9-x}\text{La}_x\text{Th}_{0.1}$ . Open triangles:  $x=0.06$ , solid triangles:  $x=0.094$ . Open circles:  $x=0.115$ , solid circles:  $x=0.14$ .

$\chi T$  vs  $T/T_0$  is independent of  $x$ . In this case, however, the scaling breaks down for  $T > T_0$ . The breakdown of the single-parameter scaling in this system is thought to be due to the large renormalization of the energy parameters which occurs at  $T_0$  because of the change in volume.

At high temperatures, the susceptibility becomes Curie-Weiss-like for all  $x$ , having the dependence  $\chi(T) = C/(T + \theta)$  where  $\theta$  is the paramagnetic Curie temperature. The measured Curie constant  $C$  is independent of  $x$  and corresponds to a cerium moment of  $2.47\mu_B$ , which is in reasonable agreement with the value of  $2.45\mu_B$  quoted for pure  $\alpha$ -cerium.<sup>11</sup> Lattice constant measurements from neutron diffraction measurements performed in the present study indicate that the valence at room temperature is also independent of  $x$  and is the same as that for pure  $\gamma$ -cerium. The values of  $\theta$

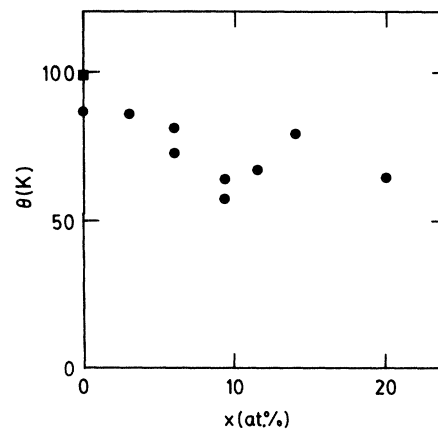


FIG. 6. Curie-Weiss  $\theta$  values as defined in text as a function of concentration. Circles: this study, square: from Ref. 16.

shown in Fig. 6 display some scatter but little variation as a function of  $x$ . Hence, we conclude that the macroscopic behavior of the high-temperature state is not significantly affected by the addition of lanthanum to the system.

#### IV. NEUTRON SCATTERING

##### A. Experimental details

The neutron-scattering experiments were performed at the Brookhaven National Laboratory high-flux beam reactor on a triple-axis spectrometer. The spectrometer was operated in the constant- $Q$  mode of operation with a fixed analyzer energy of 30 meV and varying incident energy. This mode of operation is convenient since no corrections to the observed intensities due to changes in the instrumental resolution are needed as the energy varies.<sup>20</sup> The horizontal collimation was 40', 20', 40', and 40' between the reactor and monochromator, the monochromator and sample, the sample and analyzer, and the analyzer and detector, respectively. The monochromator and analyzer consisted of pyrolytic graphite crystals aligned for the (002) reflection. The above configuration resulted in a resolution of 2.4 meV at zero energy transfer increasing to 3.2 meV at an energy transfer of 15 meV. Each data point was normalized to the counts of a monitor detector placed between the monochromator and the sample to account for fluctuations in beam intensity.

##### B. Elastic scattering and form factor study

Four polycrystalline  $\text{Ce}_{0.9-x}\text{La}_x\text{Th}_{0.1}$  samples with  $x=0.14, 0.20, 0.40,$  and  $0.90$  were studied. The latter was used to establish the nonmagnetic background. Elastic scans were performed as a function of momentum transfer  $Q$  at room temperature for all four samples and also at liquid-helium temperature for the Ce-containing samples. This was for the purpose of monitoring sample quality, i.e., crystalline phase homogeneity, and also of determining if magnetic order was present at low temperature. As discussed in Sec. II, these scans showed only fcc peaks with a small contribution from an fcc impurity. There was no indication of magnetic order in the three samples which were run at low temperature.

The lattice constant was measured as a function of temperature using a series of elastic scans performed at several temperatures between 4.2 and 200 K. These consisted of short scans,

$2.06 \leq Q \leq 2.17 \text{ \AA}^{-1}$ , in steps of  $0.005 \text{ \AA}^{-1}$  through the (111) peak in the diffraction pattern. The results are shown in Fig. 7. Also shown for comparison are the lattice constant measurements<sup>8</sup> made on  $\text{Ce}_{0.74}\text{Th}_{0.26}$ . These measurements indicated that even at the lowest temperatures, these samples are only weakly mixed valent. Assuming that the measured lattice constant depends linearly on the concentration,  $a = (0.9-x)a_{\text{Ce}} + xa_{\text{La}} + 0.1a_{\text{Th}}$ , and that the cerium lattice constant depends linearly on the valence,  $a_{\text{Ce}} = (4-\eta)a_{\text{Ce}^{3+}} + (\eta-3)a_{\text{Ce}^{4+}}$ , leads to estimates of the  $T=0$  valence of  $\eta_0 = 3.2 \pm 0.1, 3.1 \pm 0.1,$  and  $3.0 \pm 0.1$  for  $x=0.14, 0.20,$  and  $0.40,$  respectively. These estimates<sup>8</sup> assume that  $a_{\text{Ce}^{3+}} = 5.221 \text{ \AA}$  and  $a_{\text{Ce}^{4+}} = 4.661 \text{ \AA}$  and include a small correction for normal expansion.

In order to determine the  $Q$  dependence of the magnetic scattering, we have performed a constant energy scan on the  $\text{Ce}_{0.76}\text{La}_{0.14}\text{Th}_{0.1}$  sample at an energy transfer which is beyond the phonon cutoff. Under the assumption that the only  $Q$  dependence arises from the magnetic form factor [i.e.,  $S^{zz}(Q, \omega)$  is independent of  $Q$ , see below] this provides a measure of the magnetic form factor of the system.

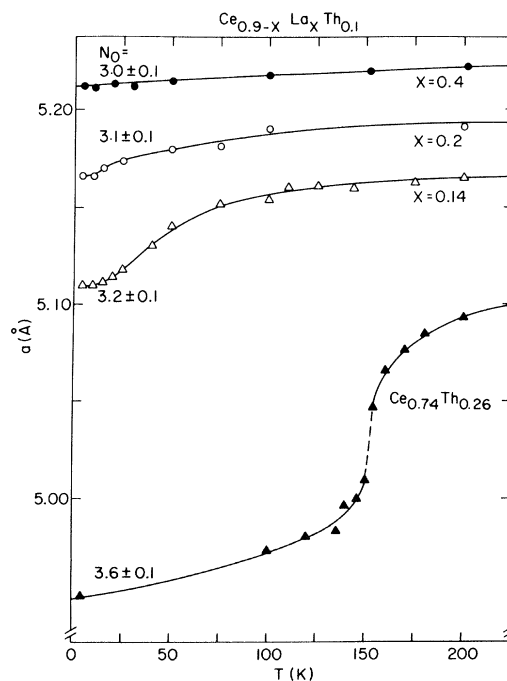


FIG. 7. Plot of the lattice constant vs temperature for the three samples containing cerium and for the  $\text{Ce}_{0.74}\text{Th}_{0.26}$  alloy studied in Ref. 8. The valence at low temperature as determined from Vegard's law is indicated for each sample.

The measurement was performed at  $T=110$  K at an energy transfer of 15 meV. The results are shown in Fig. 8. The solid line is the best fit to the square of the  $\text{Ce}^{3+}$  form factor given by Lander and Brun.<sup>21</sup> The fit seems to be reasonable. A similar result was obtained<sup>8</sup> for  $\text{Ce}_{0.74}\text{Th}_{0.26}$ .

### C. Inelastic scattering

#### 1. Determination of phonon background

In all neutron scattering studies of magnetic scattering of polycrystalline materials, it is necessary to correct for phonon background. This is usually done by comparing observed spectra with that of a nonmagnetic sample which is expected to have a similar phonon density of states. We have used the  $\text{La}_{0.9}\text{Th}_{0.1}$  sample for this purpose. Scans at only a few temperatures were required since it is well known that the scattered intensity for inelastic nuclear scattering, due to phonons, is proportional to

$$n(\omega) + 1 = (1 - e^{-\beta\hbar\omega})^{-1}, \quad (2)$$

where  $\hbar\omega = \Delta E$  and  $\beta = (kT)^{-1}$ . The different temperature scans were needed to confirm this proportionality. The phonon spectra from the  $\text{La}_{0.9}\text{Th}_{0.1}$  sample, scaled by  $[n(\omega) + 1]^{-1}$ , are shown in Fig. 9. The data for the three temperatures were averaged and smoothed slightly to give the values used for the phonon correction (solid line).

The phonon spectrum is expected to be basically the same throughout the  $\text{Ce}_{0.9-x}\text{La}_x\text{Th}_{0.1}$  alloy system since the crystal structure is the same for

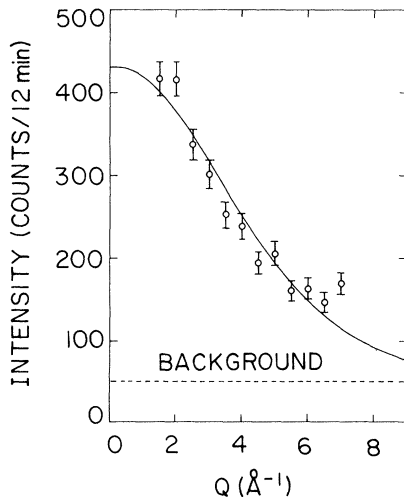


FIG. 8. Neutron scattering cross section as a function of momentum transfer at  $\hbar\omega = 15$  meV for the  $\text{Ce}_{0.76}\text{La}_{0.14}\text{Th}_{0.1}$  sample at  $T = 110$  K. Solid line: fit to square of  $\text{Ce}^{3+}$  form factor as discussed in text.

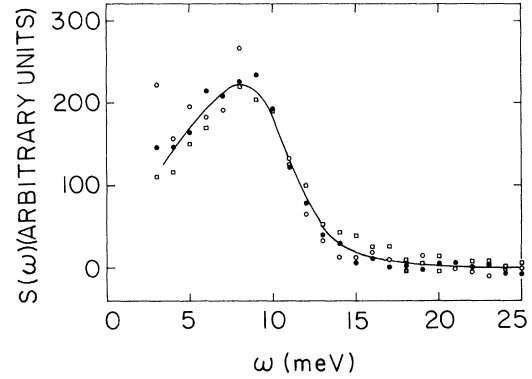


FIG. 9. Inelastic neutron scattering spectra for the  $\text{La}_{0.9}\text{Th}_{0.1}$  alloy corrected for a constant background and multiplied by  $[n(\omega) + 1]^{-1}$ . Open circles:  $T = 4.5$  K, closed circles:  $T = 50$  K, squares:  $T = 110$  K, solid line: smoothed average of the three spectra.

all  $x$ , the lattice constant change is small, and cerium and lanthanum have very similar masses. There is evidence that mixed valence leads to a marked softening of certain phonon modes<sup>22</sup> which would affect the details of the phonon scattering; however, there is no evidence of a measurable change in the phonon spectrum in this system. For the momentum transfer probed, the magnetic contribution is larger than the nuclear contribution at all temperatures in all three of the cerium samples as can be seen at the top of Fig. 10, and, since any changes in the nuclear scattering would be expected to be small, experimental uncertainties may make such effects unobservable. Support for the above subtraction procedure comes from the scaling of the resulting spectra at the two different  $Q$  values. The phonon contribution increases approximately as  $Q^2$  while the magnetic scattering decreases with  $Q$  in the manner dictated by the local  $4f$  form factor. Thus, any phonon contributions not accounted for by the above procedure should be made evident by scaling the resulting spectra and comparing their shapes for a given sample and temperature. There is excellent agreement at all temperatures between the spectra taken at the two different  $Q$  values and so we see no evidence for the failure of our phonon subtraction procedure.

#### 2. Previous studies

Previous inelastic neutron scattering studies in mixed valent systems have shown results quite different from those of the present study; e.g., in studies of  $\text{Ce}_{0.74}\text{Th}_{0.26}$ ,<sup>8</sup>  $\text{CePd}_3$ ,<sup>9</sup> and  $\text{YbCu}_2\text{Si}_2$ ,<sup>23</sup> no sharp excitations have been observed which could be attributed to CEF excitations. Instead, a

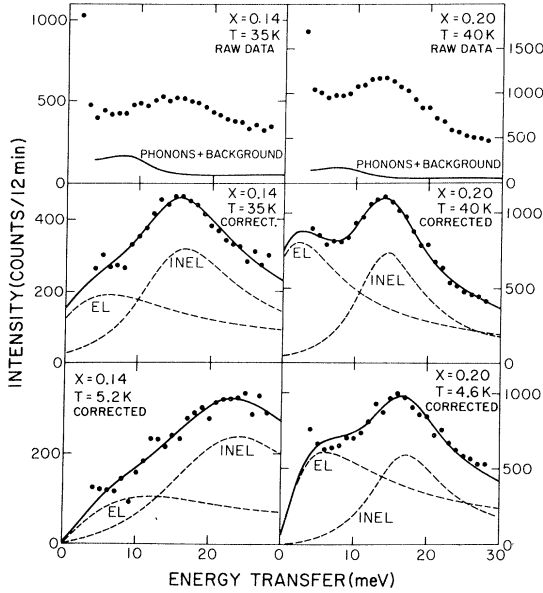


FIG. 10. Inelastic neutron spectra of  $\text{Ce}_{0.9-x}\text{La}_x\text{Th}_{0.1}$  for  $x=0.14$  and  $0.20$  taken at  $q=1.5 \text{ \AA}^{-1}$ . Top panels: raw data together with (constant) background and phonon contribution (see text). Lower panels: corrected data after subtraction of phonon and background contributions, solid lines: least-squares fit of Eq. (7), dashed lines: quasielastic (EL) and inelastic (INEL) contributions.

broad, rather featureless structure was observed which could be characterized by a single Lorentzian centered at  $\hbar\omega = \Delta E = 0$ . A sharp excitation has been observed<sup>23</sup> at approximately 10 meV in TmSe. Recent single-crystal measurements,<sup>24</sup> indicate that this is not the result of a CEF excitation, but may result from excitations across a gap formed by the hybridization of the localized  $4f$  level with the conduction band.<sup>25</sup>

The magnetic neutron scattering cross section in a cubic paramagnet can be written<sup>26</sup>

$$\frac{d^2\sigma}{d\Omega d\omega} = \left[ \frac{\gamma e^2 g}{2m_e c^2} \right]^2 \frac{k_f}{k_i} |f(\vec{Q})|^2 2S^{zz}(\vec{q}, \omega), \quad (3)$$

where  $f(\vec{Q})$  is the magnetic form factor which is the Fourier transform of the spatial part of the wave function,  $S^{zz}(\vec{q}, \omega)$  is a spin-spin correlation function, and the rest of the symbols are constants which have their usual meanings.  $S^{zz}(\vec{q}, \omega)$  can be written

$$S^{zz}(\vec{q}, \omega) = \frac{1}{2\pi} \int dt \sum_{\vec{r}} e^{i(\vec{q}\cdot\vec{r} - \omega t)} \langle S_0^z(0) S_{\vec{r}}^z(t) \rangle \quad (4)$$

$$= \frac{2\hbar}{g^2 \mu_B^2} [n(\omega) + 1] \chi'''(\vec{q}, \omega), \quad (5)$$

where  $\chi'''(\vec{q}, \omega) = \text{Im}[\chi^{zz}(\vec{q}, \omega)]$ . The spectra of the mixed valent systems mentioned above were fit by using

$$\chi'''(\vec{q}, \omega) = \chi(T) \frac{\hbar\omega\gamma}{(\hbar\omega)^2 + \gamma^2}, \quad (6)$$

where  $\chi(T)$  is the static susceptibility and  $\gamma$  is the fitting parameter, characterizing the half width at half maximum of the inelastic distribution. This form corresponds to a case where the spin dynamics are purely relaxational. The linewidth  $\gamma$  is assumed to represent the spin relaxation rate. In  $\text{CePd}_3$ ,<sup>9</sup> this linewidth is independent of temperature and approximately 20 meV. In  $\text{Ce}_{0.74}\text{Th}_{0.26}$ ,<sup>8</sup> the data could be described by the same shape of spectrum at fixed temperature, but the temperature dependence of  $\gamma$  was quite different, because of the presence of the valence transition at  $T_0 \sim 150 \text{ K}$ .

### 3. Results

Inelastic neutron scattering spectra for  $\text{Ce}_{0.9-x}\text{La}_x\text{Th}_{0.1}$  samples are shown in Fig. 11 at nearly the same temperature. A peak is observed at a finite energy for each  $x$  in contrast to the results in other mixed valent systems. Figure 10 shows the temperature dependence of the spectra for two of the samples. The lower two curves for each sample have been corrected for phonon and background contributions. In contrast to  $\text{CePd}_3$  and  $\text{Ce}_{0.74}\text{Th}_{0.26}$ , these spectra cannot be described by a single quasielastic line.

The  $\text{Ce}^{3+}$   $J = \frac{5}{2}$  ground state is split by a cubic CEF into two levels, a  $\Gamma_7$  doublet ground state and a  $\Gamma_8$  quartet. If these levels were well defined and separated by an energy  $\Delta$  large compared to the widths of the levels, the scattering would be characterized by two Lorentzians centered at  $\hbar\omega = \pm\Delta$ , in addition to the quasielastic peaks centered at  $\hbar\omega = 0$ . The intensities of these peaks would be described by the transition matrix elements and population factors of the two levels. However, in the present system, the linewidth is not small compared to  $\Delta$  and the correct functional form for the cross section can be obtained only by inversion of the complete dynamical matrix.<sup>27</sup> In addition, when the valence is also fluctuating, properly accounting for the population factors is equivalent to completely solving the Anderson lattice problem. Because of these difficulties, we assumed a generalized form of the cross section to fit the data

$$\chi''(\omega, T) = \hbar\omega \left[ A(T) \left[ \frac{\gamma}{(\hbar\omega)^2 + \gamma^2} \right] + B(T) \left[ \frac{\gamma}{(\hbar\omega - \Delta)^2 + \gamma^2} + \frac{\gamma}{(\hbar\omega + \Delta)^2 + \gamma^2} \right] \right]. \quad (7)$$

Fits using this form are shown as solid lines in Fig. 11 and in the lower sections of Fig. 10, and the temperature dependences of the linewidth  $\gamma$  and CEF splitting  $\Delta$  are shown in Fig. 12. The dashed lines in Fig. 10 show the quasielastic (labeled EL) and the inelastic (labeled INEL) contributions from Eq. (7).

The use of Eq. (7) for the fits restricts the  $\Gamma_7$  and  $\Gamma_8$  levels to have the same width,  $\gamma$ . Allowing each of them to have a different width corresponds to replacing the single quasielastic line by two lines with widths  $\gamma_1$  and  $\gamma_2$  each of which must be allowed to have a different intensity, and replacing  $\gamma$  by  $(\gamma_1 + \gamma_2)/2$  in the two inelastic Lorentzians. This introduces two more fitting parameters, bringing the total to 6. Unfortunately, six parameters

proved to be too many to determine accurately. The four parameter fits to Eq. (7) seem to describe the scattering very well.

A check on the fitting procedure can be made by comparing the static susceptibility as measured using the Faraday method to that calculated from the fits. The static susceptibility can be calculated using the Kramers-Kronig relations

$$\chi'(0, T) = \int_{-\infty}^{\infty} d\omega \frac{\chi''(\omega, T)}{\omega}. \quad (8)$$

Substitution of Eq. (7) into the above results in

$$\chi'(0, T) = \pi\hbar[A(T) + 2B(T)]. \quad (9)$$

Since no attempt was made to convert the data to absolute cross-section units, Eq. (9) gives the susceptibility in arbitrary units. These curves were then scaled to best fit the data taken by the Faraday method. The results are shown in Fig. 13. There is excellent agreement in the temperature dependences obtained by the two methods, leading us to conclude that our fitting procedure is adequate. This method of determining  $\chi'(0, T)$  sup-

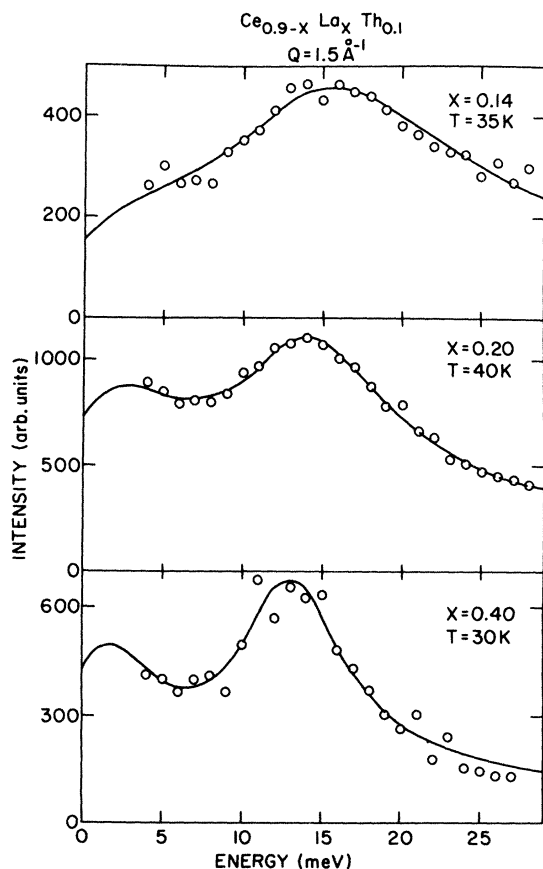


FIG. 11. Inelastic scattering spectra for the three samples at approximately the same temperatures. The appearance and narrowing of the inelastic peak in the spectrum can be seen.

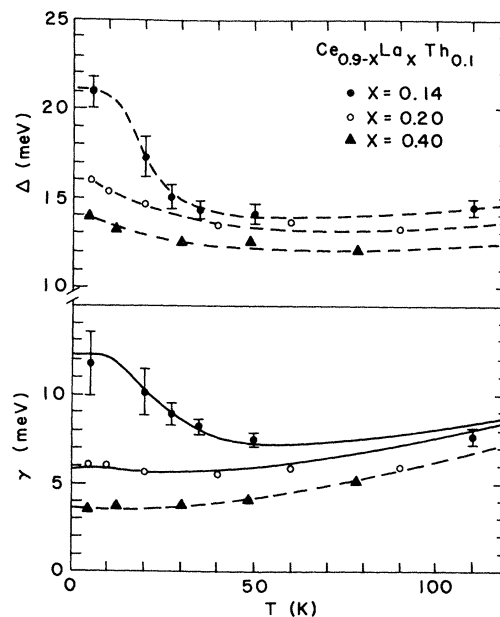


FIG. 12. Temperature dependence of CEF splitting  $\Delta$  and neutron scattering linewidth  $\gamma$  for  $\text{Ce}_{0.76}\text{La}_{0.14}\text{Th}_{0.10}$ ,  $\text{Ce}_{0.70}\text{La}_{0.20}\text{Th}_{0.10}$ , and  $\text{Ce}_{0.5}\text{La}_{0.4}\text{Th}_{0.1}$ . Solid lines: plots of  $kC_0/2\chi(T)$ , where  $\chi(T)$  is the static susceptibility. Dashed lines: guides to the eye.



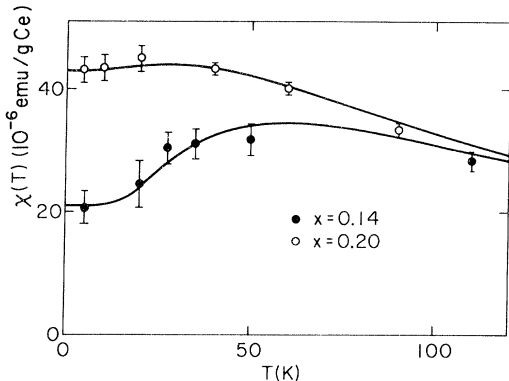


FIG. 13. Solid lines: static susceptibility measured by the Faraday method for two of the  $\text{Ce}_{0.9-x}\text{La}_x\text{Th}_{0.1}$  samples. Points: static susceptibility derived from fits to Eq. (7) as discussed in text, scaled to fit Faraday method measurements.

ports the assumption presented in Sec. III A that the upturns observed at low temperature in the static susceptibility are due to impurities rather than intrinsic effects. Magnetic impurities which interact very weakly with each other can be considered as a paramagnet with a very small Curie temperature and will therefore contribute<sup>28</sup> only to the scattering near  $\Delta E=0$ , well below the lower energy cutoff of 4 meV employed in the data analysis.

## V. DISCUSSION

The presence of the CEF transitions in the spectra provide the first measurement of the CEF splitting in fcc cerium. As mentioned above, no CEF transitions have been observed in mixed valent systems previously. All of the systems studied before had a linewidth  $\gamma \gtrsim 20$  meV, which is large compared to the expected CEF splitting of  $\sim 10$  meV. If the CEF levels exist in these systems, it would be difficult to separate the scattering due to the CEF transitions from the quasielastic scattering if the crystal-field levels are also broadened.

A second possible explanation for the lack of observable CEF transitions, other than the difficulties discussed above, may be the lack of CEF splitting in these systems. When the spin lifetime is short (i.e.,  $\gamma$  is larger) the  $f$  electron does not remain in its state long enough to feel the effects of the CEF. By alloying with lanthanum, we can increase the lifetime until CEF effects become important, and the transitions can be observed.

The anomalously large increase in  $\Delta$  as  $T$  is decreased (Fig. 12) is difficult to understand. In the

case of trivalent fcc cerium with  $J = \frac{5}{2}$ , the point-charge model gives  $\Delta \propto q_{\text{eff}}/a^5$  where  $a$  is the lattice constant of the system. Using the relation

$$q_{\text{eff}} \propto \bar{\eta} = 0.76\eta_{\text{Ce}} + 0.14\eta_{\text{La}} + 0.10\eta_{\text{Th}},$$

the average valence, and the measured lattice constant, results in a value for  $\Delta$  which is 35% smaller than the observed value at  $T=5.3$  K when  $\Delta$  is normalized to agree with the measured value at  $T=110$  K. A possible explanation for this large increase in  $\Delta$  focuses on the instantaneous symmetry of the cerium sites. As the fluctuation rate increases, the probability of finding a site with an instantaneous local symmetry which is not perfectly cubic increases. This increases the various multipole contributions to the splitting.

The basic behavior of the linewidth is as expected. At high temperatures, it is roughly constant and as the sample is cooled through the valence transition,  $\gamma$  increases rapidly, becoming constant again at low temperature. Since the valence increases in the same region, as shown by the lattice constant measurements shown in Fig. 7, we expect the spin lifetime to decrease, resulting in an increase in  $\gamma$ . Since the valence change is greatest in the 14 at. % sample, the increase in  $\gamma$  is largest here, too. In general, when the mixed valent nature of the system increases, the linewidth increases. This is seen in the behavior of  $\gamma$  with both  $x$  and  $T$ .

Generally, the quasielastic linewidth is inversely proportional to the static susceptibility. To investigate this, we have compared  $\gamma$  to  $\chi^{-1}$  as a function of temperature. The results are shown as the solid lines of Fig. 12. A least-squares fit results in the relationship

$$\gamma(T) = \frac{C_0 k}{2\chi(T)}, \quad (10)$$

where  $k = (11.6 \text{ K/meV})^{-1}$  is Boltzmann's constant. This implies that the relevant coefficient is temperature and concentration independent for  $T \lesssim 75$  K and equal to  $C_0 k/2$ . If  $\gamma$  represents the energy of the spin fluctuations, we can also write  $\gamma = kT_{\text{SF}}$  where  $T_{\text{SF}}$  is the spin-fluctuation temperature; whereupon, Eq. (10) can be written

$$\chi(T) = \frac{C_0}{2T_{\text{SF}}(T)}. \quad (11)$$

Equation (11) is identical in form to the relationship observed by Lawrence and Murphy<sup>29</sup> for the  $\text{CeIn}_{3-x}\text{Sn}_x$  system (for which  $T_{\text{SF}}$  is essentially temperature independent), if  $T_{\text{SF}}$  is defined as the

TABLE I. Valence and energy-related parameters of the mixed valent ground state.  $C_0=5760 \mu\text{emu K/g Ce}$  is the Curie constant for noninteracting cerium atoms.

	$\eta_0$	$5.6T_0$ (K)	$C_0/2\chi_0$	$\gamma/k$ (K)	
$\text{Ce}_{0.74}\text{Th}_{0.26}$ <sup>a</sup>	$3.6 \pm 0.1$	840	778	$812 \pm 85$	( $T=140$ K) <sup>b</sup>
$\text{Ce}_{0.76}\text{La}_{0.14}\text{Th}_{0.10}$	$3.2 \pm 0.1$	134	136	$136 \pm 21$	( $T=5.3$ K)
$\text{Ce}_{0.70}\text{La}_{0.20}\text{Th}_{0.10}$	$3.1 \pm 0.1$	67	67	$71 \pm 3$	( $T=4.6$ K)
$\text{Ce}_{0.50}\text{La}_{0.40}\text{Th}_{0.10}$	$3.0 \pm 0.1$		32	$42 \pm 3$	( $T=4.5$ K)

<sup>a</sup>Reference 8.

<sup>b</sup>The valence transition is essentially complete at 140 K as determined by lattice constant measurements.

temperature where the susceptibility falls to one half the free-ion value. The latter definition is equivalent to setting  $T_{\text{SF}}$  equal to  $\theta$  in the observed Curie-Weiss behavior,  $\chi \propto (T + \theta)^{-1}$ . Similar correspondences can be seen in other reported studies of Ce- and Yb-bases systems.<sup>30</sup>

We have at our disposal three independent ways of determining  $T_{\text{SF}}(0)$  for the  $\text{Ce}_{0.9-x}\text{La}_x\text{Th}_{0.1}$  system: (1) the measured linewidth  $\gamma$  in the inelastic neutron scattering experiments  $T_{\text{SF}}(0) \equiv \gamma/k$ , (2) Eq. (11):  $T_{\text{SF}}(0) = C_0/2\chi_0$ , (3) Eq. (10) combined with the observed relation  $\chi_0 \equiv \chi(0) = C_0/11.2T_0$  (see Sec. III A), which results in  $T_{\text{SF}}(0) = 5.6T_0$ . Table I compares the energies measured in each of the three ways for the samples which were examined in the neutron scattering experiments. The agreement is excellent.

The results in Table I pose interesting questions regarding charge fluctuations versus spin fluctuations. Since neutrons do not couple directly to charge fluctuations, the observed broadening  $\gamma$  of

the quasielastic peak in the neutron spectra is strictly a measure of the spin-fluctuation energy. On the other hand, it would seem that the valence transition temperature  $T_0$  should be related in some manner to the charge-fluctuation energy. Thus, it is puzzling that the spin-dependent quantities  $\chi_0^{-1}$  and  $\gamma$  should exactly track  $T_0$ . There appear to be only two possible conclusions: (1) that the charge-fluctuation energy exactly tracks the spin-fluctuation energy even as the valence is widely varied, or (2) that the charge-fluctuation energy in the ground state is independent of the valence-transition temperature.

#### ACKNOWLEDGMENTS

This research was supported in part by the Division of Basic Energy Sciences, U.S. Department of Energy, under Contract No. DE-AC02-76CH00016 and in part by the National Science Foundation, under Grant No. DMR-8005099.

\*Present address: Physics Department, Brookhaven National Laboratory, Upton, New York 11973.

<sup>1</sup>See, e.g., the following conference proceedings, along with reviews cited in Refs. 2–4: *Valence Instabilities and Related Narrow Band Phenomena*, edited by R. D. Parks (Plenum, New York, 1977).

<sup>2</sup>C. M. Varma, *Rev. Mod. Phys.* **48**, 219 (1976).

<sup>3</sup>D. I. Khomski, *Sov. Phys. Usp.* **22**, 879 (1980) [*Usp. Fiz. Nauk* **129**, 443 (1979)].

<sup>4</sup>J. M. Robinson, *Phys. Rep.* **51**, 1 (1979).

<sup>5</sup>L. L. Hirst, *Phys. Kondens. Mater.* **11**, 255 (1970).

<sup>6</sup>C. M. Varma and Y. Yafet, *Phys. Rev. B* **13**, 2950 (1976).

<sup>7</sup>E. Holland-Moritz, M. Loewenhaupt, W. Schmatz, and

D. K. Wohlleben, *Phys. Rev. Lett.* **38**, 983 (1977).

<sup>8</sup>S. M. Shapiro, J. D. Axe, R. J. Birgeneau, J. M. Lawrence, and R. D. Parks, *Phys. Rev. B* **16**, 2225 (1977).

<sup>9</sup>E. Holland-Moritz, D. Wohlleben, and M. Loewenhaupt, *J. Phys. (Paris)* **39**, C6-835 (1978).

<sup>10</sup>Preliminary reports of the present study appear in B. H. Grier, S. M. Shapiro, C. F. Majkrzak, and R. D. Parks, *Phys. Rev. Lett.* **45**, 666 (1980).

<sup>11</sup>As in the case of elemental cerium in the fcc phase, for a review of the properties of elemental cerium, see D. C. Koskenmaki and G. A. Gschneider, Jr., in *Handbook on the Physics and Chemistry of Rare Earths*, edited by K. A. Gschneider, Jr., and

- L. Eyring (North-Holland, Amsterdam, 1978), p. 337.
- <sup>12</sup>R. T. Weimer, W. E. Freeth, and G. V. Raynor, *J. Instrum. Met.* **86**, 185 (1957).
- <sup>13</sup>J. D. Greiner and J. F. Smith, *Phys. Rev. B* **4**, 3275 (1971).
- <sup>14</sup>F. H. Spedding and J. J. Croat, *J. Chem. Phys.* **59**, 2451 (1973).
- <sup>15</sup>K. A. Gschneider, Jr., Ref. 1, p. 89.
- <sup>16</sup>J. M. Lawrence, Thesis (University of Rochester, 1977) (unpublished).
- <sup>17</sup>R. A. Elenbaas, C. J. Schinkel, and E. Swakman, *J. Phys. F* **9**, 1261 (1979).
- <sup>18</sup>M. A. Manheimer and R. D. Parks, *Phys. Rev. Lett.* **42**, 321 (1979); M. A. Manheimer, Thesis (University of Rochester, 1978) (unpublished).
- <sup>19</sup>J. Lawrence, *Phys. Rev. B* **20**, 3770 (1979).
- <sup>20</sup>N. J. Chesser and J. D. Axe, *Acta Crystallogr. A* **29**, 160 (1973).
- <sup>21</sup>G. H. Lander and T. O. Brun, *J. Chem. Phys.* **53**, 1387 (1970).
- <sup>22</sup>H. A. Mook, R. M. Nicklow, T. Penney, F. Holtzberg, and M. W. Shafer, *Phys. Rev. B* **18**, 2925 (1978); H. A. Mook and R. M. Nicklow, *ibid.* **B 20**, 1656 (1979); N. Wakabayashi, *ibid.* **B 22**, 5833 (1980).
- <sup>23</sup>M. Loewenhaupt and E. Holland-Mortiz, *J. Appl. Phys.* **50**, 7456 (1979).
- <sup>24</sup>B. H. Grier and S. M. Shapiro, in *Valence Fluctuations in Solids*, edited by L. M. Falicov, W. Hanke, and M. B. Maple (North-Holland, Amsterdam, 1981), pp. 325–1328.
- <sup>25</sup>A. J. Fedro and S. K. Sinha, in Ref. 24.
- <sup>26</sup>W. Marshall and S. W. Lovesey, in *Theory of Thermal Neutron Scattering* (Oxford, Oxford, 1971).
- <sup>27</sup>K. W. Becker, P. Fulde, and J. Keller, *Z. Phys. B* **28**, 9 (1977).
- <sup>28</sup>P. G. De Gennes, *J. Phys. Chem. Solids.* **4**, 223 (1958).
- <sup>29</sup>J. Lawrence and D. Murphy, *Phys. Rev. Lett.* **40**, 961 (1978).
- <sup>30</sup>J. C. P. Klaasse, W. C. M. Mattens, F. R. DeBoer, and P. F. DeChatel, *Physica (Utrecht)* **86–88 B**, 234 (1977).